ACS APPLIED MATERIALS & INTERFACES

www.acsami.org

Research Article

Phone Camera Nano-Biosensor Using Mighty Sensitive Transparent Reusable Upconversion Paper

Kamaljit Kaur, Bandana Kumari Sahu, Kanchan Swami, Mahima Chandel, Anshika Gupta, Li-Hua Zhu, Jeffrey P. Youngblood,* Selvaraju Kanagarajan,* and Vijayakumar Shanmugam*

Cite This: *ACS Appl. Mater. Interfaces* 2022, 14, 27507−27514

Read Online

ACCESS | Metrics & More | Article Recommendations | Supporting Information

ABSTRACT: Lycopene, a natural colorant and antioxidant with a huge growing market, is highly susceptible to photo/thermal degradation, which demands real-time sensors. Hence, here a transparent upconversion nanoparticles (UCNPs) strip having 30 mol % Yb, 0.1 mol % Tm, and β-$NaYF_4$ UCNPs, which shows an intense emission at 475 nm, has been developed. This strip has been found to be sensitive to lycopene with a detection limit as low as 10 nM using a smartphone camera, which is due to static quenching that is confirmed by the lifetime study. In comparison to previous paper strips, here the transparent strip has minimal scattering with maximum sensitivity in spite of not using any metal quenchers. An increase in strip hydrophobicity during the fabrication process complements the strip to selectively permeate and present an extraction-free substitute analysis for chromatography. Hydrophobicity endows the strip with the capability to reuse the strip with ∼100% luminescence recovery.

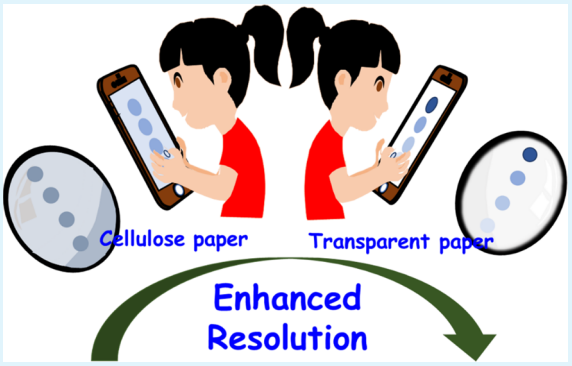

KEYWORDS: *UCNPs, sensing, lycopene, tomato, CNC film*

INTRODUCTION

Lycopene, the natural colorant and antioxidant, is becoming an important constituent in the food and beverage, nutraceutical, pharmaceutical, and cosmetics industries. Its market was $66 million in 2010, which increased to $107 million in 2020 and is expected to reach $200 million in 2030.[1,2] It is an expensive natural compound extracted predominantly from tomatoes, and the cost can go above $6000 kg^{-1}. Lycopene has been found to reduce the risk of cardiac diseases, cancers, organ disorders, metabolic syndrome, and infertility,[3,4] which emphasizes its role as a nutraceutical in human health.[5−8] Importantly, the poorest consumer group of the population has been found to be in the need of lycopene supplement,[9] and supplement in different forms like juice, soup, and sauce has shown the plasma lycopene content to increase by ∼60% (up to 1.15 $\mu M\ L^{-1}$).[10] Latest regulation in the food industry emphasizes the labeling of the ingredient to differentiate natural from artificial ingredients.[11] The concentration of lycopene in turn controls the flavor as it is the precursor for the high odor unit value compound 6-methyl-5-hepten-2-one.[12] Lycopene is susceptible to light, temperature, and microbial degradation, which warrants high throughput sensing at various stages from raw material purchase to processing to the supply chain, etc. Lycopene is acyclic with 5, 9, 13, and 15 position isomers having three absorbance maxima between 400 and 510 nm, which draws special attention for having the highest reactive oxygen removal rate among all carotenoids (Kq: $31 \times 10^9\ M^{-1}\ S^{-1}$).[13,14]

The cutting-edge technology to control the optical properties in nanoparticles led to the development of optical sensors for metal ions and the quantification of organic molecules.[15−17] Such detection is based on fluorescence and absorbance energy transfer (ET), static/dynamic quenching mechanism, and fluorescence resonance energy transfer (FRET)/inner filter effect.[18] Other mechanisms like electron/hole annealing, aggregation-induced quenching/emission, and chroma response have been explored for fluorescence change and colorimetric detection.[19−22] Recent developments in fluorescence-assisted detection use machine learning to analyze the curve pattern and identify the nucleotide.[23] The ubiquitous access to smartphones gives the convenience of sensor integration like the piezo etc., for on-the-spot analysis.[24] Similarly, the use of smartphone camera sensors has been developed for the quantification of metal, glucose, antibiotics, covid virus, etc.[25−30] On the other hand, in the search for more versatile, low-cost, and reusable sensors, paper-based platforms

Received: April 19, 2022
Accepted: May 17, 2022
Published: June 6, 2022

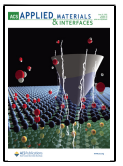

are encouraged.[31] Similarly, fabric-based calorimetric signals are emerging as a user-friendly technique.[32] Very recently, excellent sensor paper for thiram detection as low as 60 nM concentration in fruits and vegetables has been fabricated using fluorescent carbon quantum dots having intense blue emission.[33]

Among fluorescent nanoparticles, near-infrared (NIR)-sensitive materials have gained more attention as they are free from background interference.[34,35] In plant metabolite quantification, samples rich in chromophores often show background fluorescence in visible light excitation.[36−38] Hence, the intense fluorescence upconversion nano-biosensor paper (upconversion nanoparticles (UCNPs)) with NIR excitation could be a possible solution with smartphone camera-assisted documentation. Such UCNPs based smart phone camera is comparatively limited to few demonstrations like drug counterfeiting and quantification of pesticide in fruits and other samples.[39−41]

In this study, we developed an upconversion sensor paper having high transparency to detect lycopene levels with high precision using the overlap of lycopene absorbance with the UCNPs emission coupled with a smartphone camera-assisted quantification. To our knowledge, for the first time, here upconversion sensor paper of high transparency with low scattering has been developed in contrast to cellulose papers with regular scattering. The transparent paper has been optimized by us previously for other packing applications.[42] Also, the increase in the hydrophobicity during cellulose nanocrystal (CNC) modification and UCNPs addition paves the way for efficient lycopene mobility and quenching. Further, this also gives accessibility to the solvent, to wash all of the lycopene pockets after use, to restore ∼100% emission, which has again not demonstrated previously. As agricultural products are highly perishable and the level of antioxidants fluctuates at the fruit maturation stage, these kinds of real-time sample analysis are needed to speed up the detection and reduce the dependence on lengthy and costly chromatographic analysis in food quality control processes.

MATERIALS AND METHODS

The chemicals and materials used in this study were as follows: octadecene, oleic acid (Sigma-Aldrich), yttrium acetate (Sigma-Aldrich), ytterbium acetate (Sigma-Aldrich), thulium acetate (Sigma-Aldrich), acetone, methanol (high-performance liquid chromatography (HPLC) grade), water (HPLC grade), hexane (Merck), 2,6-di-*tert*-butyl 4-methyl phenol (Sigma-Aldrich), methyl *tert*-butyl ether (MTBE) (Sigma HPLC grade), lycopene (Sigma-Aldrich), poly(vinyl alcohol) (PVA) (molecular weight (MW) 89,000−98,000), cellulose nanocrystals (provided by Forest Products Lab Batch 2018-FPL-CNC-130, 10.0 wt % in water, 1.06 wt % sulfur on dry CNC, sodium form), C30 column (YMC), ascorbic acid (Sigma-Aldrich), glucose (HiMedia), naringenin (HiMedia), magnesium sulfate (Thermo Fisher), sodium carbonate (Merck), calcium hydroxide (Merck), potassium nitrate (HiMedia), quinoline yellow (TCI), and chlorogenic acid (HiMedia).

Characterization. Powder X-ray diffraction (PXRD) analysis was carried out in a Bruker ADVANCE D8 diffractometer that has a Cu Kα radiation source (λ = 1.5406 Å) at 40 kV and 25 mA. Transmission electron microscopy and high-resolution transmission electron microscopy (HRTEM) were performed using a JEOL-JEM 2100 with a lanthanum hexaboride filament at an accelerating voltage of 200 kV. The photoluminescence spectra were measured using a FluoroMax-4 spectrofluorometer (Horiba) equipped with 980 nm laser excitation. The contact angle was measured using a Kruss ADVANCE drop shape analyzer. HPLC was performed in a Waters instrument having MTBE and 95% methanol as the mobile phase and C30 (YMC 250 × 4.6 mm^2 I.D.) column in a gradient flow as the stationary phase. Ellipsometer studies were performed on an Angstrom Sun Technologies Inc. TF probe to determine the film thickness and wavelength at 633 nm.

Synthesis of β-NaYF$_4$, 30 mol % Yb, and 0.1 mol % Tm Upconversion Nanoparticles. The synthesis has been followed with the aim to achieve the maximum UCNPs emission intensity that can have overlap at the wavelength of lycopene absorbance maxima. For this, the precursor ratio of the activator and emitter were changed while following the rest of the steps as reported previously.[43] Briefly, in a 50 mL three-neck flask, Y$(CH_3COO)_2$, Yb(CH_3COO_2), and Tm(CH_3COO_2) with 2.8, 1.2, and 0.02 mM precursor concentrations, respectively, were prepared in 7:3 ratio of octadecene and oleic acid. The temperature of this mixture was increased to 120 °C in vacuum and kept in continuous stirring for 30 min. The reaction temperature was reduced to ∼50 °C, followed by the addition of 16 mM NH_4F and a 10 mM NaOH solution prepared in methanol. Once the solution turned turbid, it was allowed to stir for 30 min. The methanol was then removed from the reaction using vacuum at 90 °C. Finally, the temperature was further increased to 300 °C with constant stirring for 1.5 h.

After cooling, the UCNPs were precipitated by the addition of 40 mL of acetone to the resultant solution, followed by centrifugation at 7000 rpm for 10 min. The resultant pellet was washed using a hexane/ethanol mixture a minimum of three times, and the resultant pellet was then redispersed in hexane and stored for further use.

Upconversion Luminescence Quenching in Solution with Lycopene Addition. Using fixed concentrations of upconversion nanoparticles (0.5 mg mL^{-1}), the quenching efficiency (QE) of the luminescence was measured with increasing lycopene concentrations from 80 pM to 2 μM. Here, the maximum titration volume was 10 μL, which does not have luminescence attenuation. A 980 nm laser was used as the excitation source.

Interference Study. Fruits commonly contain ethanol, ascorbic acid, glucose, naringenin, magnesium, sodium, calcium, potassium, quinolone yellow, and chlorogenic acid; hence, these molecules were considered as the model compounds for an interference study of UCNPs quenching. These molecules were added to the UCNPs solution in a similar volume to arrive at an equimolar lycopene concentration, and the emission spectra of UCNPs were measured using 980 nm excitation wavelength.

Fluorescence Quenching in Real Sample Analysis. In case of real sample analysis, different concentrations of tomato juice were added to an optimum concentration of UCNPs (0.5 mg mL^{-1}) and centrifuged at 9000 rpm for 10 min. The supernatant was discarded and the remaining pellet was resuspended in the same volume of hexane, and the emission spectra were measured at 980 nm excitation wavelength.

Time-Resolved Decay Measurements. Lifetime decay measurements of UCNPs were carried out both in the presence and absence of lycopene using 980 nm laser as excitation source for an emission wavelength at 475 nm. The curves were fitted to single exponentials, and the average lifetime was calculated.

Sensor Paper Strip Fabrication. The CNC/PVA paper strip was fabricated using our previous protocol optimized to maximum transparency.[42] Briefly, 11.9 g of PVA powder was added to 88 mL of water and stirred at 85 °C. This PVA solution was mixed with CNCs at a ratio of 0.3:0.7. This mixture was sonicated and stirred for another 2 h, following which it was cast onto glass slides. Approximately, 1.5 ml of the above CNC/PVA aliquot was shear-cast at an angle of 45° using a single-edge razor blade. The shear-casting was repeated approximately three to four times on the glass slide, and the slide was incubated in a desiccator for 4−6 days. After this time, the paper strips were peeled off from the glass slide and stored in a controlled atmosphere at room temperature for further use. A similar protocol was followed for UCNPs cast paper strip fabrication by adding 2 mg mL^{-1} UCNPs in the CNC/PVA suspension.

https://doi.org/10.1021/acsami.2c06894
ACS Appl. Mater. Interfaces 2022, 14, 27507−27514

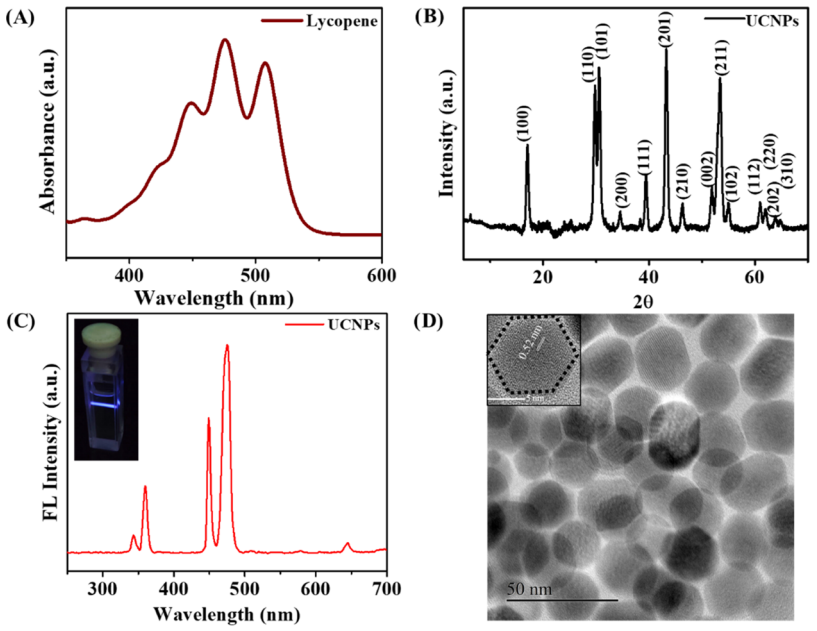

Figure 1. (A) UV−vis absorbance spectra of lycopene. (B) XRD pattern of as-prepared $NaYF_4$, Yb^{3+}, and Tm^{3+} UCNPs matching with JCPDS 16-0334. (C) Photoluminescence spectra of as-prepared UCNPs and inset showing a photograph of as-prepared UCNPs when irradiated using a 980 nm excitation laser. (D) TEM and HRTEM images of UCNPs showing a lattice *d*-spacing of 0.52 nm.

Lycopene Content Validation in a Real Sample Using HPLC. Lycopene was extracted and analyzed using HPLC. Briefly, tomato juice was dehydrated using 65 mL of methanol, followed by filtration through a glass Buchner funnel.[44] The filtrate was mixed with a mixture of carbon tetrachloride and methanol in a separating funnel to extract the lycopene to the organic phase and repeated three times. Then, a few drops of hot methanol and benzene were added to the resultant before solvent evaporation and redispersed into hexane for further analysis.

HPLC analysis was carried out using MTBE:95% methanol as the mobile phase and C30 as the stationary column using a PDA detector having 400−530 nm as the detection wavelength. Lycopene standards were injected for the calibration plot.

Contact Angle Measurement. The contact angle was measured on a dried paper strip using a drop shape analyzer (Kruss advance drop shape) equipped with a high-resolution charge-coupled device (CCD) camera. A small rectangular sensor paper strip was placed on the sample holder, a drop was placed onto the surface of the sensor paper strip, and the contact angle was measured.

Image Analysis. A simple in-house system was fabricated to house the laser and sensor paper strip at different compatible positions for smartphone camera (OnePlus 8T; Qualcomm Snapdragon 865 chipset)-assisted imaging. The fabricated sensor paper strips were peeled off from the substrate after drying and cut into 0.5 cm × 0.5 cm pieces. The laser was illuminated at an angle of 45° with respect to the paper strip position, and a NIR filter was placed in front of the camera, which was vertically above the sensor paper strip. Different dilutions of lycopene were added to the fabricated sensor paper strip, and images were captured using a OnePlus 8T smartphone camera. Further images were analyzed using ImageJ software, and the respective blue intensity was measured at the desired area.

Real Sample Analysis Using the Sensor Paper Strip. Real sample analysis was performed on sensor paper strips by diluting tomato fruit juice 10 times and adding 10 μL of diluted juice onto the sensor paper strip. Following this, the strips were air-dried and imaged using the smartphone camera for image analysis.

RESULTS AND DISCUSSION

This study aimed to develop an upconversion sensor paper to quantify the lycopene present in fruits and vegetables. The lycopene has absorbance maxima at 475 nm (Figure 1A); hence, to detect this, UCNPs with the emission maxima in the same range have been synthesized and characterized with minor modifications. From the literature, it was clear that this emission arises from a band corresponding to the $^1G_4 \rightarrow {}^3H_6$ transition from the Tm^{3+} activator in the $NaYF_4$ host having Yb^{3+} as the sensitizer. Further, the ratio of Yb^{3+} and Tm^{3+} has to be optimized to avoid cross-relaxation and nonradiative loss, which may compromise the desired maximum of 475 nm emission.[45−47] Therefore, UCNPs with different Yb^{3+} and Tm^{3+} ratios were synthesized with Yb^{3+} at 30% and varying Tm^{3+} ion concentrations by the thermal decomposition method reported by us previously for the vitamin D fortification in mushrooms.[48]

Synthesized UCNPs were characterized using XRD and emission spectrophotometry at 980 nm excitation. The XRD pattern confirms the presence of hexagonal β-$NaYF_4$ phase material by matching with the JCPDS standard card 16-0334 (Figure 1B). In the case of emission spectra, the UCNPs with 0.1% Tm^{3+} exhibited an emission maximum at 475 nm, which was 9 times larger than the 650 nm emission (Figure 1C). The photograph of the UCNPs illuminated by the 980 nm NIR laser at 2 W is given in Figure 1C inset, contrary to our previous study that shows 475 nm emission ∼2 times the 650 nm emission while having 30% Yb^{3+} with 0.5% Tm^{3+}. Thus, this material with the maximum emission at 475 nm qualifies for the high sensitivity by maximum quenching at a minimum lycopene concentration. The TEM image of the sample with the selected emission spectra shows the average particle size to be 25 nm (Figure 1D). The HRTEM image of the particles shows the "*d*" spacing between the lattice to be 0.52 nm (Figure 1D inset), which corresponds to the (100) hexagonal phase of $NaYF_4$ host nanocrystals.

Spectroscopic Analysis. Before the sensor paper fabrication, the suitability of the nanoparticles to show luminescence quenching through energy transfer (ET) by the overlap of the UCNP emission with the lycopene

https://doi.org/10.1021/acsami.2c06894
ACS Appl. Mater. Interfaces 2022, 14, 27507−27514

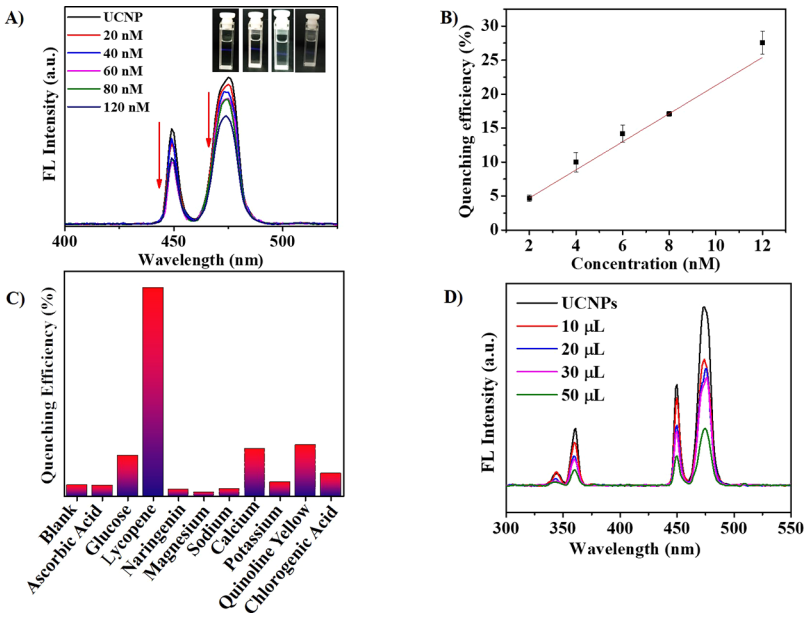

Figure 2. (A) Fluorescence quenching of UCNPs on the addition of different lycopene concentrations (nM); inset shows the corresponding fluorescence photo. (B) Linear calibration plot showing fluorescence quenching efficiency (%) at different lycopene concentrations (nM). (C) Quenching efficiency with other possible interfering molecules in fruit juice shows the selectivity of the material to lycopene. (D) Real sample analysis showing an increase in gradual fluorescence quenching in proportion to the increase in the fruit juice concentration.

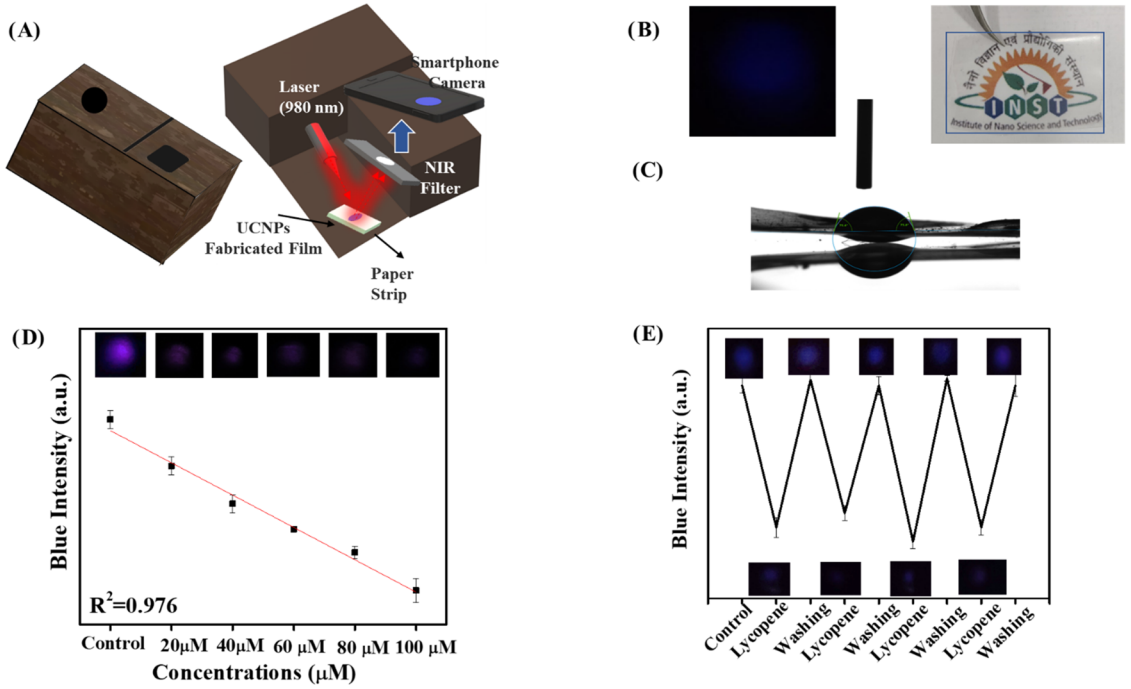

Figure 3. (A) Image of in-house custom-designed accessory with a cross-sectional view for smartphone/laser housing. (B) Luminescence image of the as-prepared UCNPs sensor paper strip under 980 nm laser excitation captured using a smartphone camera. (Left) Photograph of the as-prepared UCNPs-embedded transparent sensor paper strip showing the transparency of the strip on the institute emblem (right). (C) Contact angle measurement of the UCNP-embedded sensor paper strip. (D) Luminescence image of the UCNP sensor paper strip with the addition of increasing lycopene concentrations. (Red line depicts the linear fit of the sensor paper strip to the increasing lycopene concentration.) (E) Reusability of the UCNP sensor paper strip shown with the luminescence image restoration with each washing (corresponding normalized blue intensity is plotted).

absorbance has been examined. Different UCNPs concentrations were titrated with 10 μM lycopene and found that 0.5 mg mL^{-1} UNCP was suitable to show measurable quenching efficiency. Following this, the fluorescence stability and maximum quenching signal of the UCNPs in response to lycopene concentrations were determined in different solvents like hexane, tetrahydrofuran (THF), toluene, benzene, ether, and chloroform. Here, benzene, ether, and chloroform showed aggregation; hence, the fluorescence signals were poor, whereas in THF and toluene, the quenching was not

https://doi.org/10.1021/acsami.2c06894
ACS Appl. Mater. Interfaces 2022, 14, 27507−27514

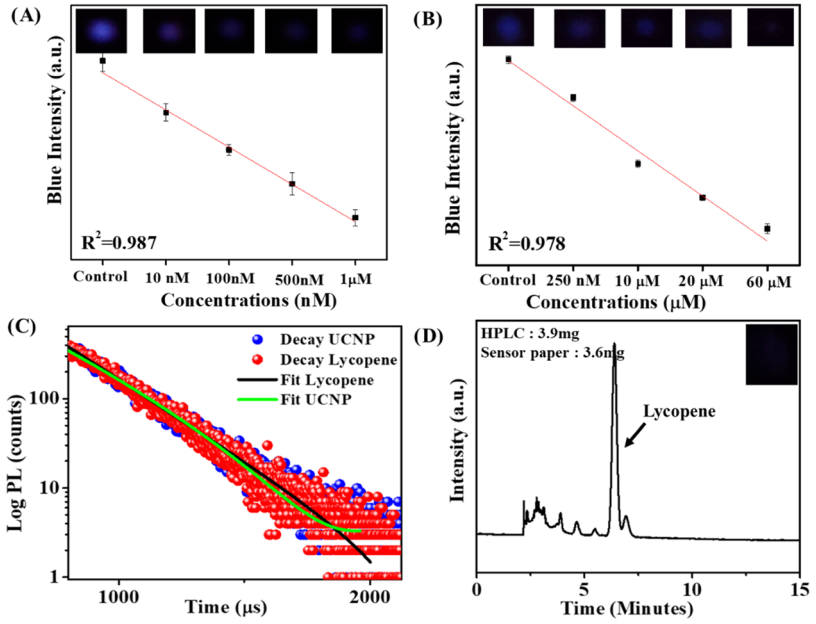

Figure 4. (A) Limit of detection optimization of a transparent UCNPs sensor paper strip showing a linear plot of quenching efficiency as low as 10 nM lycopene. (B) Limit of detection optimization of a UCNPs sensor paper strip prepared on regular cellulose paper. (C) Lifetime analysis of UCNPs fluorescence decay in the presence and absence of lycopene with its corresponding fit. (D) Representative HPLC spectra of extracted lycopene in a C30 column and inset showing real sample analysis on the transparent strip.

proportional (Figure S2). In hexane, lycopene concentration-dependent quenching of 450 and 475 nm UCNP emission peak with a detection limit of 80 pM lycopene to 120 nM using 0.5 mg mL^{-1} UCNPs was observed (Figure 2A, B). This optimization of UCNP concentration allowed us to reach a detection limit of 80 pM (Figure S3). The same amount of blank solvent was titrated in 0.5 mg mL^{-1} UCNPs to ensure the absence of quenching by the solvent. (Figure S4). Here, the UCNPs did not show any measurable quenching with the addition of control solvent without lycopene, which confirms that the quenching is due to the analyte addition.

Quenching efficiency was calculated with respect to each analyte according to the equation

$$\text{QE}\ (\%) = I_0 - I/I_0$$

where I_0 is the fluorescence intensity before and I is the fluorescence intensity after the addition of the analyte.

Ultimately, the aim of the study was to use this sensor design for real sample analyses, specifically for fruit quality determination, which have the major constituents like ethanol, ascorbic acid, glucose, naringenin, magnesium, sodium, calcium, potassium, and chlorogenic acid. So, to ensure the selectivity of 450 and 475 nm peak quenching to lycopene, the effect of the above compounds that belong to sugar, alcohol, vitamins, polyphenols, and ions along with artificial food colorant quinolone yellow was investigated at μM concentration and found to have no interference (Figures 2C and S5–S13). After this confirmation, real sample analysis was pursued using tomato juice, which is rich in lycopene. Figure 2D shows that with an increase in the real sample concentration, there is a proportional decrease in the 450 and 475 nm emission intensity of UCNPs, which has not been observed in the control addition. The proportional reduction in the 350 nm peak may be due to the minor absorbance in the lycopene.

Transparent UCNP Sensor Paper Strip Preparation and Characterization. With the above encouraging results that show the UCNPs to be sensitive and selective to ~pM concentration of lycopene, a transparent UNCPs sensor paper strip was optimized with the aim of highest sensitivity. To fabricate such a sensor, a 98% transparent paper optimized by us using cellulose nanocrystals (CNCs) and PVA (due to the matching refractive index)[38] was tested with different amounts of UCNPs. The luminescence image of the fabricated UCNPs paper was captured using a smartphone placed in such a way that the camera fits the window of an in-house custom-designed accessory (Figure 3A). This accessory holds a 980 nm portable laser at an angle of 45° with respect to the sensor paper at a convenient distance along with the band pass filter placed in front of the smartphone camera. The CNC + PVA composite with 2 mg mL^{-1} UCNPs was found suitable for maximum transparency and optimum luminescence at 450 mW of laser power (Figure 3B). To ensure that the composite containing UCNPs has the same elasticity as that of our previous CNC/PVA mixture,[42] the loss and storage modulus has been measured. The composite results showed ~3.5 times improvement in the storage modulus than that of the CNC/PVA mixture, thereby proving it to have more elasticity, which may be due to the role of UCNPs as a reinforcement agent (Figure S14). The higher concentration of UCNPs causes intense emission that becomes insensitive to the low analyte concentration, whereas a lower concentration does not cause detectable emission. Therefore, the UCNPs concentration was optimized to 2 mg mL^{-1}, so that it has readability as low as 10 μM lycopene quenching in the smartphone camera.

The prepared sensor strip is desired to have a hydrophobic surface to have high lycopene mobility; therefore, the water contact angle of the strip was measured. The contact angle measurement shows that the contact angle of the sensor paper increased to 80° (Figure 3C) from 40° in the UCNPs-free transparent paper (40° can be referred from our previous publication, which is also a significant increase compared to the regular cellulose paper). This increase may be due to the

https://doi.org/10.1021/acsami.2c06894
ACS Appl. Mater. Interfaces 2022, 14, 27507−27514

complementary effect from the oleic acid coating on the as-prepared UNCPs, which is desired to enhance the hydrophobic interaction with lycopene.

Quantification of the Sensitivity. The UCNPs sensor paper strip in Figure 3D shows the luminescence quenching sensitive to a proportional increase in the lycopene concentration when illuminated with a 980 nm portable laser at 450 mW. The numerical count of the blue channel was measured using ImageJ software. Following this, to check the suitability of the UCNPs sensor strip to be reused multiple times, the sensor strip was quenched with the maximum amount of lycopene, i.e., 100 μM was washed with hexane and tested if the blue channel count was restored at every washing. In this experiment, for five repetitions, the sensor strip was shown to restore the luminescence to the original value each time (Figure 3E). The transparent paper was found compatible since it is comparatively hydrophobic and thus allows the hexane to reach all of the micropores to wash away the hydrophobic lycopene. To check the stability of the strip, the thickness of the strip was measured using an ellipsometer, which showed the thickness to be stable at ∼1700 nm (Figure S15a,b).

Further, to compare the limit of detection of the transparent strip with that of the regular cellulose filter paper, which is commonly used, an equal amount of optimum concentration of UCNPs was dropped on both materials and tested against lycopene. The strips were titrated with a reducing nM concentration of lycopene, showing the limit of detection of the transparent sensor strip to be 10 nM (Figure 4A), whereas the regular cellulose filter paper with the UCNPs cast showed the detection limit to be 250 nM (Figure 4B). This improvement in detection may be due to lower scattering in the transparent paper that allows the maximum blue channel count to reach the camera, whereas in the regular paper, the quenching limit of the trace is undetected due to scattering. Thus, in the regular paper, to improve the limit of detection, metal or strong organic dye with a high absorbance index is needed.

Sensing Mechanism behind the Limit of Detection. To understand the mechanism behind quenching, the UCNPs fluorescence lifetime was measured. In fluorescence lifetime measurement, τ_{avg1} is the UCNP lifetime, i.e., ∼0.23 ms, and the τ_{avg2} is the UCNPs lifetime after lycopene addition, i.e., ∼0.238 ms (Figure 4C). There was no significant change in the lifetime, and hence, the τ_{avg1}/τ_{avg2} was nearly 1, which confirms that the ET is static rather than dynamic.[49,50] This means there is a spectral overlap between the UCNPs emission and lycopene absorbance range, and fluorescence quenching is due to an inner filter effect. This is a vital phenomenon of a spectrofluorometer as it does not require any particular orientation of fluorophores and quenchers. Therefore, ET occurs by the completion of fluorescence emission and reabsorption. The dynamic ET occurs only if there is a nonradiative transfer of energy from the donor to the acceptor, which occurs with the close proximity of the donor and acceptor that is recommended for photodynamic applications.

In this condition, the regular cellulose paper that causes scattering of the emission may not give enough emission for metal-free molecules, which suffer from poor quenching coefficients to cause significant quantifiable quenching at low concentrations. Further, the hydrophobicity of the fabricated sensor paper strip may also have allowed the analyte to reach closer to effective quenching at low concentrations. Although the donor/acceptor distance is a minor factor in the static quenching, it cannot be ignored with a significant increase in the contact angle.

Real Sample Analysis and Luminescence Quenching Mechanism. The evidence observed above shows that the sensor strip method developed may not require sample extraction, as the emission peak and the hydrophobicity are selective to the lycopene. Hence, for the real sample analysis, tomato juice was diluted to tenfolds, since the sensor strip is highly sensitive with a detection limit in the range 10 nM. This may be due to the ability of the NIR excitation to overcome the background autofluorescence. Thus, diluted samples showed concentration-dependent quenching, which has been crosschecked using the HPLC (Figure 4D). The reading was very close, with a difference of ∼7%.

CONCLUSIONS

Lycopene is an important carotenoid with the highest antioxidant potential and its quantification is gaining more importance in the food and agriculture industry. A portable smartphone camera-based cost-effective UCNPs sensor strip with a detection limit of 10 nM free of metal quenchers has been developed, which has better resolution compared to other recently published excellent studies (Table 1). Due to the use of a smartphone and nanopaper-based sensor, the method can be used with little to no skill. The sensitivity of detection is significantly higher than that of a regular cellulose paper, probably due to the minimum scattering in the transparent paper. The strip also shows ∼100% luminescence recovery with simple washing, allowing for reusability, which renders the strips convenient for the Internet of things-assisted data pooling from different locations, which is emphasized for future agriculture.[51]

Table 1. Performance Comparison with Previous Publication of Upconversion Paper Using Quenching and Recovery Principles

analyte	reference	minimum concentration
thiram (thiram copper complex as a quencher)	41	100 μM
sulfite	39	60 nM
cocaine with gold nanoparticles as quenchers	52	5 nM
fluoride ion (complex formation using curcumin)	53	5 μM
no metal quenchers	present work	10 nM

ASSOCIATED CONTENT

Supporting Information

The Supporting Information is available free of charge at https://pubs.acs.org/doi/10.1021/acsami.2c06894.

Optimization of solvents for sensing lycopene, interference study, ellipsometry study for the nanocomposite film, and rheology studies for the nanocomposite (Figures S1−S15) (PDF)

AUTHOR INFORMATION

Corresponding Authors

Jeffrey P. Youngblood − *School of Materials Engineering, Purdue University, West Lafayette, Indiana 47907, United*

https://doi.org/10.1021/acsami.2c06894
ACS Appl. Mater. Interfaces 2022, 14, 27507−27514

States; orcid.org/0000-0002-8720-8642; Email: jpyoungb@purdue.edu

Selvaraju Kanagarajan − *Department of Plant Breeding, Swedish University of Agricultural Sciences, 234 22 Lomma, Sweden;* orcid.org/0000-0003-4341-9322; Email: selvaraju.kanagarajan@slu.se

Vijayakumar Shanmugam − *Institute of Nano Science and Technology, Mohali, Punjab 140306, India;* orcid.org/0000-0001-7117-5631; Email: vijayakumarshanmugham@gmail.com, psvijayakumar@inst.ac.in

Authors

Kamaljit Kaur − *Institute of Nano Science and Technology, Mohali, Punjab 140306, India*

Bandana Kumari Sahu − *Institute of Nano Science and Technology, Mohali, Punjab 140306, India*

Kanchan Swami − *Institute of Nano Science and Technology, Mohali, Punjab 140306, India*

Mahima Chandel − *Institute of Nano Science and Technology, Mohali, Punjab 140306, India*

Anshika Gupta − *Institute of Nano Science and Technology, Mohali, Punjab 140306, India*

Li-Hua Zhu − *Department of Plant Breeding, Swedish University of Agricultural Sciences, 234 22 Lomma, Sweden*

Complete contact information is available at: https://pubs.acs.org/10.1021/acsami.2c06894

Notes

The authors declare no competing financial interest.

■ ACKNOWLEDGMENTS

K.K. is thankful to CSIR for the fellowship. V.S. thanks the Department of Science and Technology, Science and Engineering Research Board (DST-SERB), Government of India (CRG/2019/006317), and DBT (BT/PR36476/NNT/28/1723/2020). The authors are grateful to Prof. Prakash P. Neelakandan and Dr. Siddharth Tiwari for fruitful discussion on fluorescence interpretation and HPLC measurement respectively.

■ REFERENCES

(1) Ciriminna, R.; Fidalgo, A.; Meneguzzo, F.; Ilharco, L. M.; Pagliaro, M. Lycopene: Emerging Production Methods and Applications of a Valued Carotenoid. *ACS Sustainable Chem. Eng.* **2016**, *4*, 643−650.

(2) Lycopene Market by Form, Nature, and Application: Global Opportunity Analysis and Industry Forecast, 2021−2030. https://www.researchandmarkets.com/reports/5457282/lycopene-market-by-form-nature-and-application#src-pos-4 (accessed Jan 28, 2022).

(3) Pereira Soares, N. d. C.; Teodoro, A. J.; Oliveira, F. L.; Takiya, C. M.; Junior, A. P.; Nasciutti, L. E.; Lotsch, P. F.; Granjeiro, J. M.; Ferreira, L. B.; Pereira Gimba, E. R.; Borojevic, R. Lycopene Induce Apoptosis in Human Prostate Cells and Alters the Expression of Bax and Bcl-2 Genes. *LWT—Food Sci. Technol.* **2014**, *59*, 1290−1297.

(4) Fernández-García, E. Skin Protection Against UV light by Dietary Antioxidants. *Food Funct.* **2014**, *5*, 1994−2003.

(5) Giovannucci, E.; Ascherio, A.; Rimm, E. B.; Stampfer, M. J.; Colditz, G. A.; Willett, W. C. Intake of Carotenoids and Retinol in Relation to Risk of Prostate Cancer. *J. Natl. Cancer Inst.* **1995**, *87*, 1767−1776.

(6) Giovannucci, E.; Rimm, E. B.; Liu, Y.; Stampfer, M. J.; Willett, W. C. A Prospective Study of Tomato Products, Lycopene, and Prostate Cancer Risk. *J. Natl. Cancer Inst.* **2002**, *94*, 391−398.

(7) Wu, H.; Pan, H.; Li, Z.; Liu, T.; Liu, F.; Xiu, S.; Wang, J.; Wang, H.; Hou, Y.; Yang, B.; Lei, L.; Lian, J. Efficient Production of Lycopene from CO_2 via Microbial Electrosynthesis. *Chem. Eng. J.* **2022**, *430*, No. 132943.

(8) Di Mascio, P.; Kaiser, S.; Sies, H. Lycopene as the Most Efficient Biological Carotenoid Singlet Oxygen Quencher. *Arch. Biochem. Biophys.* **1989**, *274*, 532−538.

(9) Jenab, M.; Ferrari, P.; Mazuir, M.; Tjonneland, A.; Clavel-Chapelon, F.; Linseisen, J.; Trichopoulou, A.; Tumino, A.; Bueno-de-Mesquita, H. B.; Lund, E.; Gonzalez, C. A.; Johansson, G.; Key, T. J.; Riboli, E. Variations in Lycopene Blood Levels and Tomato Consumption across European Countries Based on the European Prospective Investigation into Cancer and Nutrition (EPIC) Study. *J. Nutr.* **2005**, *135*, No. 2032S.

(10) Grainger, E. M.; Hadley, C. W.; Moran, N. E.; Riedl, K. M.; Gong, M. C.; Pohar, K.; Schwartz, S. J.; Clinton, S. K. A Comparison of Plasma and Prostate Lycopene in Response to Typical Servings of Tomato Soup, Sauce or Juice in Men before Prostatectomy. *Br. J. Nutr.* **2015**, *114*, 596−607.

(11) Food additives defined as per EU Regulation EC 1333/2008.

(12) Berna, A. Z.; Lammertryn, J.; Saevels, S.; Di Natale, C.; Nicolaï, B. M. Electronic Nose Systems to Study Shelf Life and Cultivar Effect on Tomato Aroma Profile. *Sens. Actuators, B* **2004**, *97*, 324−333.

(13) Miller, E. S.; Mackinney, G.; Zscheile, F. P. Absorption Spectra of Alpha and Beta Carotenes and Lycopene. *Plant Physiol.* **1935**, *10*, 375−381.

(14) Grabowska, M.; Wawrzyniak, D.; Rolle, K.; Chomczyński, P.; Oziewicz, S.; Jurga, S.; Barciszewski, J. Let Food Be Your Medicine: Nutraceutical Properties of Lycopene. *Food Funct.* **2019**, *10*, 3090−3102.

(15) Balbinot, S.; Srivastav, A. M.; Vidic, J.; Abdulhalim, I.; Manzano, M. Plasmonic Biosensors for Food Control. *Trends Food Sci. Technol.* **2021**, *111*, 128−140.

(16) Swarnkar, A.; Shanker, G. S.; Nag, A. Organic-Free Colloidal Semiconductor Nanocrystals as Luminescent Sensors for Metal Ions and Nitroaromatic Explosives. *Chem. Commun.* **2014**, *50*, 4743−4746.

(17) Zare, H.; Ghalkhani, M.; Akhavan, O.; Taghavinia, N.; Marandi, M. Highly Sensitive Selective Sensing of Nickel Ions Using Repeatable Fluorescence Quenching-Emerging of the CdTe Quantum Dots. *Mater. Res. Bull.* **2017**, *95*, 532−538.

(18) Ghosh, H. N.; Pal, H.; Palit, D. K.; Mukherjee, T.; Mittal, J. P. Interaction of the Excited Singlet State of Disubstituted Anthraquinones with Aliphatic and Aromatic Amines: A Fluorescence Quenching Study. *J. Photochem. Photobiol., A* **1993**, *73*, 17−22.

(19) Han, S.; Yang, L.; Wen, Z.; Chu, S.; Wang, M.; Wang, Z.; Jiang, C. A Dual-Response Ratiometric Fluorescent Sensor by Europium-Doped CdTe Quantum Dots for Visual and Colorimetric Detection of Tetracycline. *J. Hazard. Mater.* **2020**, *398*, No. 122894.

(20) Jiang, R.; Zhang, Y.; Zhang, Q.; Li, L.; Yang, L. Carbon dot/Gold Nanocluster- Based Fluorescent Colorimetric Paper Strips for Quantitative Detection of Iodide Ions in Urine. *ACS Appl. Nano Mater.* **2021**, *4*, 9760−9767.

(21) Wang, H.; Da, L.; Yang, L.; Chu, S.; Yang, F.; Yu, S.; Jiang, C. Colorimetric Fluorescent Paper Strip with Smartphone Platform for Quantitative Detection of Cadmium Ions in Real Samples. *J. Hazard. Mater.* **2020**, *392*, No. 122506.

(22) Jiang, R.; Lin, D.; Zhang, Q.; Li, L.; Yang, L. Multiplex Chroma-Response Based Fluorescent Smartphone Sensing Platform for Rapid and Visual Quantitative Determination of Antibiotic Residues. *Sens. Actuators, B* **2022**, *350*, No. 130902.

(23) Huang, Y.; Li, Z.; Risinger, A. L.; Enslow, B. T.; Zeman, C. J.; Gong, J.; Yang, Y.; Schanze, K. S. Fluorescence Spectral Shape Analysis for Nucleotide Identification. *Proc. Natl. Acad. Sci. U.S.A.* **2019**, *116*, 15386−15391.

(24) Gil, B.; Li, B.; Gao, A.; Yang, G. Z. Miniaturized Piezo Force Sensor for a Medical Catheter and Implantable Device. *ACS Appl. Electron. Mater.* **2020**, *2*, 2669−2677.

(25) Wei, Q.; Nagi, R.; Sadeghi, K.; Feng, S.; Yan, E.; Ki, S. J.; Caire, R.; Tseng, D.; Ozcan, A. Detection and Spatial Mapping of Mercury Contamination in Water Samples Using a Smart-Phone. *ACS Nano* **2014**, *8*, 1121−1129.

(26) Chu, S.; Wang, H.; Du, Y.; Yang, F.; Yang, L.; Jiang, C. Portable Smartphone Platform Integrated with a Nanoprobe-Based Fluorescent Paper Strip: Visual Monitoring of Glutathione in Human Serum for Health Prognosis. *ACS Sustainable Chem. Eng.* **2020**, *8*, 8175−8183.
(27) Park, D. H.; Heo, J. M.; Jeong, W.; Yoo, Y. H.; Park, B. J.; Kim, J. M. Smartphone-Based VOC Sensor Using Colorimetric Polydiacetylenes. *ACS Appl. Mater. Interfaces* **2018**, *10*, 5014−5021.
(28) McLeod, E.; Wei, Q.; Ozcan, A. Democratization of Nanoscale Imaging and Sensing Tools Using Photonics. *Anal. Chem.* **2015**, *87*, 6434−6445.
(29) Jin, R.; Kong, D.; Yan, X.; Zhao, X.; Li, H.; Liu, F.; Sun, P.; Lin, Y.; Lu, G. Integrating Target-Responsive Hydrogels with Smartphone for On-Site Ppb-Level Quantitation of Organophosphate Pesticides. *ACS Appl. Mater. Interfaces* **2019**, *11*, 27605−27614.
(30) Zhang, Y.; Malekjahani, A.; Udugama, B. N.; Kadhiresan, P.; Chen, H.; M Osborne, M.; Franz, M.; Kucera, M.; Plenderleith, S.; Yip, L.; Bader, G. D.; Tran, V.; Gubbay, J. B.; McGeer, A.; Mubareka, S.; Chan, W. C. W. Surveilling and Tracking COVID-19 Patients Using a Portable Quantum Dot Smartphone Device. *Nano Lett.* **2021**, *21*, 5209−5216.
(31) Kimberly, A.; Hiyoto, M.; Fisher, E. R. Utilizing Plasma Modified SnO_2 Paper Gas Sensors to Better Understand Gas-Surface Interactions at Low Temperatures. *J. Vac. Sci. Technol., A* **2020**, *38*, No. 043202.
(32) Tenda, K.; van Gerven, B.; Arts, R.; Hiruta, Y.; Merkx, M.; Citterio, D. Paper-Based Antibody Detection Devices Using Bioluminescent BRET-Switching Sensor Proteins. *Angew. Chem., Int. Ed.* **2018**, *57*, 15369−15373.
(33) Chu, S.; Wang, H.; Ling, X.; Yu, S.; Yang, L.; Jiang, C. A Portable Smartphone Platform Using a Ratiometric Fluorescent Paper Strip for Visual Quantitative Sensing. *ACS Appl. Mater. Interfaces* **2020**, *12*, 12962−12971.
(34) Liao, M. Y.; Wu, C. H.; Lai, P. S.; Yu, J.; Lin, H. P.; Liu, T. M.; Huang, C. C. Surface State Mediated NIR Two-Photon Fluorescence of Iron Oxides for Nonlinear Optical Microscopy. *Adv. Funct. Mater.* **2013**, *23*, 2044−2051.
(35) Mendez-Gonzalez, D.; Laurenti, M.; Latorre, A.; Somoza, A.; Vazquez, A.; Negredo, A. I.; López-Cabarcos, E.; Calderón, O. G.; Melle, S.; Rubio-Retama, J. Oligonucleotide Sensor Based on Selective Capture of Upconversion Nanoparticles Triggered by Target-Induced DNA Interstrand Ligand Reaction. *ACS Appl. Mater. Interfaces* **2017**, *9*, 12272−12281.
(36) Li, J.; Wu, H.; Santana, I.; Fahlgren, M.; Giraldo, J. P. Standoff Optical Glucose Sensing in Photosynthetic Organisms by a Quantum Dot Fluorescent Probe. *ACS Appl. Mater. Interfaces* **2018**, *10*, 28279−28289.
(37) Nadort, A.; Zhao, J.; Goldys, E. M. Lanthanide Upconversion Luminescence at the Nanoscale: Fundamentals and Optical Properties. *Nanoscale* **2016**, *8*, 13099−13130.
(38) Zhan, Q.; Qian, J.; Liang, H.; Somesfalean, G.; Wang, D.; He, S.; Zhang, Z.; Andersson-Engels, S. Using 915 Nm Laser Excited Tm3+/Er3+/Ho3+-Doped NaYbF4 Upconversion Nanoparticles for in Vitro and Deeper in Vivo Bioimaging without Overheating Irradiation. *ACS Nano* **2011**, *5*, 3744−3757.
(39) Wang, J.; Zhu, Y.; Grimes, C. A.; Nie, Z.; Cai, Q. Eu,Sm,Mn-Doped CaS Nanoparticles with 59.3% Upconversion-Luminescence Quantum Yield: Enabling Ultrasensitive and Facile Smartphone-Based Sulfite Detection. *Anal. Chem.* **2018**, *90*, 8658−8664.
(40) You, M.; Lin, M.; Wang, S.; Wang, X.; Zhang, G.; Hong, Y.; Dong, Y.; Jin, G.; Xu, F. Three-Dimensional Quick Response Code Based on Inkjet Printing of Upconversion Fluorescent Nanoparticles for Drug Anti-Counterfeiting. *Nanoscale* **2016**, *8*, 10096−10104.
(41) Mei, Q.; Jing, H.; Li, Y.; Yisibashaer, W.; Chen, J.; Li, B. N.; Zhang, Y. Smartphone Based Visual and Quantitative Assays on Upconversional Paper Sensor. *Biosens. Bioelectron.* **2016**, *75*, 427−432.
(42) Nuruddin, M.; Chowdhury, R. A.; Szeto, R.; Howarter, J. A.; Erk, K. A.; Szczepanski, C. R.; Youngblood, J. P. Structure−Property Relationship of Cellulose Nanocrystal−Polyvinyl Alcohol Thin Films for High Barrier Coating Applications. *ACS Appl. Mater. Interfaces* **2021**, *13*, 12472.
(43) Yan, B.; Boyer, J.-C.; Branda, N. R.; Zhao, Y. Near-Infrared Light-Triggered Dissociation of Block Copolymer Micelles Using Upconverting Nanoparticles. *J. Am. Chem. Soc.* **2011**, *133*, 19714−19717.
(44) Ishida, B. K.; Ma, J.; Chan, B. A Simple, Rapid Method for HPLC Analysis of Lycopene Isomers. *Phytochem. Anal.* **2001**, *12*, 194−198.
(45) Wei, G.; Wang, G.; Wang, L.; Zhu, P.; Kim, R.; Qin, W. Intense Ultraviolet Upconversion Luminescence from Hexagonal $NaYF_4$:Yb^{3+}/Tm^{3+} Microcrystals. *Opt. Express* **2008**, *16*, 11907−11914.
(46) Kar, A.; Kundu, S.; Patra, A. Lanthanide-Doped Nanocrystals: Strategies for Improving the Efficiency of Upconversion Emission and Their Physical Understanding. *ChemPhysChem* **2015**, *16*, 505−521.
(47) Zhang, Y. Y.; Yang, L. W.; Xu, C. F.; Zhong, J. X.; Sun, C. Q. Sensitized Deep-Ultraviolet up-Conversion Emissions of Gd3+ via Tm3+ and Yb3+ in Hexagonal NaYF4 Nanorods. *Appl. Phys. B* **2010**, *98*, 243−247.
(48) Kaur, K.; Bindra, P.; Mondal, S.; Li, W.-P.; Sharma, S.; Sahu, B. K.; Naidu, B. S.; Yeh, C.-S.; Gautam, U. K.; Shanmugam, V. Upconversion Nanodevice-Assisted Healthy Molecular Photocorrection. *ACS Biomater. Sci. Eng.* **2021**, *7*, 291.
(49) Ding, Y.; Wu, F.; Zhang, Y.; Liu, X.; de Jong, E. M. L. D.; Gregorkiewicz, T.; Hong, X.; Liu, Y.; Aalders, M. C. G.; Buma, W. J.; Zhang, H. Interplay between Static and Dynamic Energy Transfer in Biofunctional Upconversion Nanoplatforms. *J. Phys. Chem. Lett.* **2015**, *6*, 2518−2523.
(50) Shen, Y. F.; Tsai, M. R.; Chen, S. C.; Leung, Y. S.; Hsieh, C. T.; Chen, Y. S.; Huang, F. L.; Obena, R. P.; Zulueta, M. M. L.; Huang, H. Y.; Lee, W. J.; Tang, K. C.; Kung, C. T.; Chen, M. H.; Shieh, D. B.; Chen, Y. J.; Liu, T. M.; Chou, P. T.; Sun, C. K. Imaging Endogenous Bilirubins with Two-Photon Fluorescence of Bilirubin Dimers. *Anal. Chem.* **2015**, *87*, 7575−7582.
(51) Yoon, B. K.; Tae, H.; Jackman, J. A.; Guha, S.; Kagan, C. R.; Margenot, A. J.; Rowland, D. L.; Weiss, P. S.; Cho, N. J. Entrepreneurial Talent Building for 21st Century Agricultural Innovation. *ACS Nano* **2021**, *15*, 10748−10758.
(52) He, M.; Li, Z.; Ge, Y.; Liu, Z. Portable Upconversion Nanoparticles-Based Paper Device for Field Testing of Drug Abuse. *Anal. Chem.* **2016**, *88*, 1530−1534.
(53) Liu, Y.; Ouyang, Q.; Li, H.; Zhang, Z.; Chen, Q. Development of an Inner Filter Effects-Based Upconversion Nanoparticles-Curcumin Nanosystem for the Sensitive Sensing of Fluoride Ion. *ACS Appl. Mater. Interfaces* **2017**, *9*, 18314−18321.

https://doi.org/10.1021/acsami.2c06894
ACS Appl. Mater. Interfaces 2022, 14, 27507−27514